

Beyond Load: Understanding Cognitive Effort through Neural Efficiency and Involvement using fNIRS and Machine Learning

Shayla Sharmin
shayla@udel.edu
University of Delaware
Newark, Delaware, USA

Roghayeh Leila Barmaki
rlb@udel.edu
University of Delaware
Newark, Delaware, USA

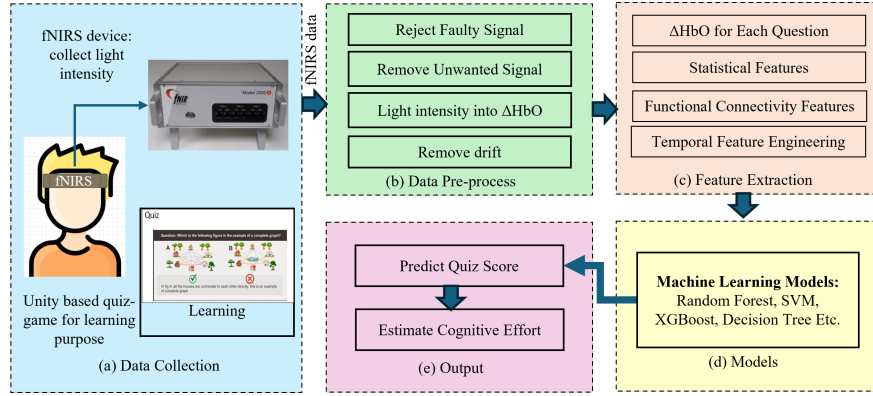


Figure 1: The overview of the proposed system (a) fNIRS data collected during quiz gameplay; (b) signals pre-processed and ΔHbO extracted; (c) statistical and connectivity features derived; Temporal feature engineering applied (d) ML models predict quiz score; (e) predicted score and ΔHbO used to estimate cognitive effort via relative neural efficiency and involvement.

Abstract

The estimation of cognitive effort could potentially help educators to modify material to enhance learning effectiveness and student engagement. Where cognitive load refers how much work the brain is doing while someone is learning or doing a task cognitive effort consider both load and behavioral performance. Cognitive effort can be captured by measuring oxygen flow and behavioral performance during a task. This study infers cognitive effort metrics using machine learning models based on oxygenated hemoglobin collected by using functional near-infrared spectroscopy from the prefrontal cortex during an educational gameplay. In our study, sixteen participants responded to sixteen questions in

an in-house Unity-based educational game. The quiz was divided into two sessions, each session consisting of two task segments. We extracted temporal statistical and functional connectivity features from collected oxygenated hemoglobin and analyzed their correlation with quiz performance. We trained multiple machine learning models to predict quiz performance from oxygenated hemoglobin features and achieved accuracies ranging from 58%–67% accuracy. These predictions were used to calculate cognitive effort via relative neural involvement and efficiency, which consider both brain activation and behavioral performance. Although quiz score predictions achieved moderate accuracy, the derived relative neural efficiency and involvement values remained robust. Since both metrics are based on the relative positions of standardized brain activation and performance scores, even small misclassifications in predicted scores preserved the overall cognitive effort trends observed during gameplay.

CCS Concepts

- **Human-centered computing** → **Human computer interaction (HCI)**;
- **Applied computing** → **Interactive learning environments**; **Learning management systems**; **Computer-assisted instruction**.

Permission to make digital or hard copies of all or part of this work for personal or classroom use is granted without fee provided that copies are not made or distributed for profit or commercial advantage and that copies bear this notice and the full citation on the first page. Copyrights for components of this work owned by others than the author(s) must be honored. Abstracting with credit is permitted. To copy otherwise, or republish, to post on servers or to redistribute to lists, requires prior specific permission and/or a fee. Request permissions from permissions@acm.org. CHI' 2026, Barcelona

© 2026 Copyright held by the owner/author(s). Publication rights licensed to ACM.

ACM ISBN 978-1-4503-XXXX-X/2018/06

<https://doi.org/XXXXXXX.XXXXXX>

Keywords

Cognitive effort, cognitive load, relative neural efficiency, relative neural involvement, performance score, functional Near-Infrared Spectroscopy (fNIRS), brain signal, hemodynamic response, educational games, machine learning,

ACM Reference Format:

Shayla Sharmin and Roghayeh Leila Barmaki. 2026. Beyond Load: Understanding Cognitive Effort through Neural Efficiency and Involvement using fNIRS and Machine Learning. In *Proceedings of CHI (CHI' 2026)*. ACM, New York, NY, USA, 10 pages. <https://doi.org/XXXXXXX.XXXXXXX>

1 Introduction

Cognitive effort (CE) refers to the level of cognitive load which is an individual experiences while learning [11, 22]. Cognitive load refers to how much the brain is working during a task [11, 17, 40]. In many cases, we see that cognitive load becomes high, but this increase alone does not clearly tell us whether the person is deeply involved in the task or struggling with it. High brain activity can occur in both situations [11, 17, 40].

This is where the idea of cognitive effort becomes useful. Unlike cognitive load, which only shows how much the brain is working, cognitive effort considers both brain activation and performance together [11, 22, 37, 39]. When both brain activity is high and performance is also good, we interpret that as involvement. But if the brain is working hard and performance is still poor, it likely reflects burden. In other words, CE helps us differentiate between productive effort and mental overload. Even when performance looks efficient, CE can reveal whether that efficiency required excessive mental strain. By combining brain load and performance, we get a clearer picture of whether the effort was manageable or overwhelming [11, 22, 37, 39].

CE is associated with increased neural activity during problem-solving, decision-making, and learning [11, 22]. When students are learning new or complex tasks, measuring CE helps us understand how hard their brains work and how to improve the design of the educational content. Relative Neural Efficiency (RNE) and Relative Neural Involvement (RNI) are two key metrics that can be used to explain CE with behavioral performance [11, 22, 33]. These metrics are derived from hemodynamic responses in the prefrontal cortex (PFC), via functional Near-Infrared Spectroscopy (fNIRS), alongside with behavioral performance. The PFC is responsible for executive functions such as decision-making, and problem-solving, which are critical in educational contexts. RNE indicates how efficiently an individual processes information and performs a task with minimal CE. Higher RNE indicates low effort and high performance, and lower RNE suggests high effort and low performance.

On the other hand, RNI measures motivation and engagement. High RNI indicates the user is more engaged and motivated during a task [11, 22, 29, 40]. A balanced RNE and RNI represents individual's engagement and efficiency during a task. Thus, understanding RNE and RNI may help to optimize learning strategies, improve engagement, and enhance cognitive performance.

Traditional methods of evaluating student efficiency and involvement rely on test assessments, self-reports, or reaction times, which are often subjective and inconsistent [7]. A few recent studies used hemodynamic responses to understand learning efficiency along with subjective measures and cognitive load [19, 27, 30]. However, CE prediction using fNIRS and machine learning models remains an open research challenge.

By applying machine learning models to estimate performance from fNIRS signals, we evaluate the possibility of estimating RNE and RNI, allowing the detection of efficient learning. Our work introduces a novel dataset, that captures both fNIRS hemodynamic responses and quiz performance score during an educational quiz game from sixteen participants. We predicted performance score using various AI models. Based on this and fNIRS data we observed cognitive effort by estimating relative neural efficiency (RNE) and involvement (RNI). Instead of optimizing only for prediction accuracy, this study emphasizes interpreting brain signal patterns to better understand cognitive effort. Our research questions (RQs) are as follows:

- RQ₁* Can machine learning models accurately predict performance scores from fNIRS-based features during educational gameplay?
- RQ₂* Can predicted performance scores from ML model reflect cognitive effort meaningfully through derived RNE and RNI metrics?

The paper is organized as follows. section 2 reviews relevant literature. section 3 outlines our experimental methodology, detailing participants, apparatus, study procedure, cognitive effort measurement methods, data acquisition procedures, pre-processing techniques, and feature extraction frame work. section 4 presents results. section 5 discusses findings about the research questions, addressing practical implications, limitations, and possible improvements. Finally, section 6 summarizes the study's findings and highlights its educational contributions.

2 Related Works

fNIRS and Machine Learning in Brain Signal Analysis: Machine learning models have been widely used on fNIRS-derived hemodynamic responses to support brain computer interface (BCI) tasks such as speech decoding [6], motor imagery [4, 26], and finger movement classification [18, 20, 28]. These models also help classify pain [8, 9] and neurological disorders like Alzheimer's [5, 21],

Parkinson's [14, 32], ADHD [41, 47], and depression [23]. Researchers have used fNIRS with ML to detect fatigue [42], estimate cognitive load [45], and classify cognitive tasks such as mental arithmetic [44, 46]. CNN and LSTM models, in particular, have achieved high accuracy. For example, Wickramaratne and Mahmud reported 87.14% accuracy in classifying arithmetic tasks using CNN [44]. Some studies combined EEG with fNIRS to improve BCI performance [6, 20, 28].

fNIRS for Cognitive Workload, Fatigue, and Performance Prediction: Beyond application in BCI and health sectors, researchers have increasingly explored how fNIRS-based models can predict cognitive workload and performance in real-world settings. fNIRS has been increasingly applied to predict cognitive workload and performance. Zhang et al. showed that DeepNet models can predict pilot workload in flight simulations using CNN-attention mechanisms[45]. Similarly, Grimaldi et al. proposed a CNN-LSTM model to predict perceptual load [12] and cognitive load [13] forecasting in piloting tasks. They stated that an LSTM-based approach demonstrated superior performance in short-term workload prediction [13]. In another study, Gado et al. classified cognitive workload in NASA task-load simulations using logistic regression [10]. Fatigue has also been investigated using fNIRS signals [10, 16, 25, 43]. In addition to workload and fatigue assessment, recent studies have explored the use of ML/DL for performance efficiency estimation, particularly in educational and learning environments. The following section discusses related works in this domain.

fNIRS in Performance and Efficiency Prediction: While most studies focus on classifying cognitive workload, researchers have also begun investigating how ML/DL can predict performance efficiency and engagement based on fNIRS signals by monitoring neural activity in different learning and task-based environments. Jeun et al. used logistic regression to predict task difficulty based on PFC activity before training. TAAfter three weeks of training, participants showed improved executive function and reduced PFC activation, indicating increased neural efficiency [19].

Pan et al. applied ML techniques to classify instructional approaches based on brain-to-brain coupling between instructors and learners. They found that machine learning models could distinguish between scaffolding-based learning and explanation-based learning better than single-brain models that highlights the role of interactive engagement in learning efficiency [30]. Another approach was proposed by Saikia, where k-means clustering has been used to classify individuals using fNIRS data during a working memory task [34]. However, the model faced challenges in generalizability due to individual differences in brain responses. Oku and Sato used fNIRS data to model with random forests and logistic

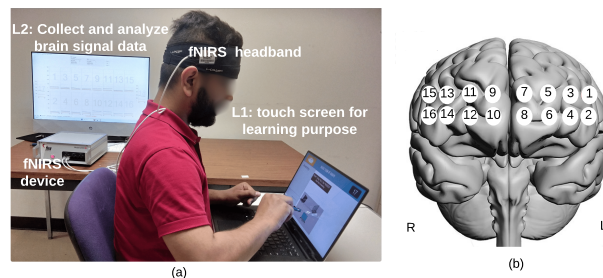


Figure 2: (a) Experimental setup: Participant playing an educational game wearing fNIRS headband. This setup captures hemodynamic responses in the prefrontal cortex, with data acquisition managed through COBI software on a secondary laptop. (b) 16 channels used for collecting ΔHbO

regression to classify student engagement and predict quiz performance in online learning platforms [27].

3 Experiment

In this section, we briefly described the data acquisition process with the user study. Later, we explained the pre-processing steps and the features we extracted.

3.1 User Study

Figure 3 represents the steps of the user study. The participants used a unity-based educational game. The game was followed Sharmin et al. provided questions [38] to evaluate participants' understanding of the basic structure of graph concepts, such as nodes, edges, loops. Throughout the study, we recorded the participants' quiz scores and hemodynamic responses from the fNIRS. The Qualtrics survey platform was used to collect responses to demographic questionnaire and pre and post-test questions. The study was approved by the institutional review board.

3.1.1 Apparatus. Figure 2 presents study setup and fNIRS headband orientation. We used two computers and an fNIRS device (Figure 2 (a)). We used an 18-channel headband fNIRS imager 2000S (fNIRS Device LLC, Potomac, MD, USA), 4 light emitters, wavelength (λ) 730-850 nm with average power < 1 mW) sampled at 10 Hz. The detectors were separated by 2.5 cm with a penetrating depth of approximately 1.2 cm. This headband was placed on participants' foreheads, and fNIRS collected data for 16 channels (Figure 2(b)). Channel 1-4 and channel 13-16 collectively called Lateral PFC (LPFC) and Channel 5-12 called Ventromedial PFC (VMPFC). Participants interacted with the educational quiz on a Dell XPS touchscreen laptop (L1) [Intel (R) Core(TM) i7-7700HQ processor at 2.80 GHz]. Another desktop computer (L2) [Intel(R) Core(TM) i7-10700T

processor at 2.00 GHz] was connected to the fNIRS device. The laptop was used to collect fNIRS data using Cognitive Optical Brain Imaging (COBI) Studio Software. We also used fNIRSoft Software (Version 4.9) to apply filters on ΔHbO data and generate CSV file for further processing.

3.1.2 Study Procedure. After signing the consent form and filling out the demographic questionnaires, the participants first experienced a demo version where the study was clearly explained and instructions about sitting still as much as possible (see Figure 3).

After completing a ten-question pre-test, they watched the recorded video tutorial where they learned the basic terminologies of the graph. In our study, we divided our 16 questions into two sessions, with each session having two segments and each segment having four questions. Participants had up to 30 seconds to answer each question, and after each question, they had five seconds of feedback. So, each segment was $140 \text{ seconds} = 4 \times 30 + 4 \times 5 = 200$ long. In between the two segments, there was a 20-second rest period. After the first session, they had a 6-10 minute break. After each session, the participants completed a post-test. We randomized the question order to minimize learning effects and control for difficulty bias across participants.

3.1.3 Cognitive Effort Measure. In this study, we aimed to estimate cognitive effort by observing the RNE and RNI in two quiz sessions. RNE represents the relationship between brain activity and task performance. While RNE measures neural efficiency, RNI measures engagement, how much voluntary effort is exerted. As each session has two segments, we have total four segments with four questions each.

To quantify cognitive effort, we first calculated the average of ΔHbO signals, representing oxygenated hemoglobin concentration, within the PFC for each learning segment. We then computed the overall group mean (GM) and standard deviation (SD) of both ΔHbO and behavioral performance scores to derive standardized z-scores [11].

Standardizing both neural and behavioral measures serves two purposes: (1) it reduces individual variability, and (2) it brings physiological effort and performance onto a common scale, enabling meaningful comparison. This z-scoring process forms the basis of RNE and RNI, which are grounded in the theoretical framework of Paas et al. [29] and extended to neuroimaging by Shewokis and Getchell [11, 22, 40].

Specifically, P_z denotes the standardized performance score, and M_z represents the standardized inverse of mean ΔHbO , based on the rationale that better learning should ideally occur with less cognitive effort. The inverse transformation of ΔHbO reflects this assumption, aligning with prior literature that interprets lower pre-frontal activation during correct performance as greater neural efficiency.

To ensure numerical stability, especially in cases where all participants performed equally and the standard deviation of the score approached zero, we added a small constant $\epsilon = 0.001$ to the denominator of the z-score formulas.

The final RNE and RNI metrics are computed using a Cartesian transformation:

$$P_z = \frac{Score_i - Score_{(GM)}}{Score_{(SD)} \cdot \epsilon} \quad (1)$$

$$CE_z = \frac{\frac{1}{\Delta HbO_i} - \frac{1}{\Delta HbO_{(GM)}}}{\frac{1}{\Delta HbO_{(SD)}}} \quad (2)$$

$$RNE = \frac{P_z - CE_z}{\sqrt{2}} \quad (3)$$

$$RNI = \frac{P_z \cdot CE_z}{\sqrt{2}} \quad (4)$$

This representation allows each participant's effort profile to be plotted in a two-dimensional space, where RNE captures efficiency (high performance, low effort), and RNI reflects involvement (combined mental effort and engagement). This approach improves the interpretability of neural data in relation to cognitive learning processes.

3.2 Data Acquisition

We collected fNIRS data using COBI, and the fNIRS recording rate was 10 samples per second. The data was saved in fNIRS format. Each question was presented for 30 seconds, so each file contained 300 rows for each question corresponding to 16 optode (ΔHbO) values. Sixteen participants answered 16 questions each, leading to 256 responses in the dataset (16×16). The dataset has 168 correct responses (class 1) and 88 incorrect responses (class 0). We used only ΔHbO because previous studies showed that ΔHbO signals are more sensitive to changes in blood flow in the participant's cortex relative to ΔHbR signals [15, 24, 31]. Since participants often answered within 20 seconds, only the first 200 rows per question were retained. The dataset contains 819,200 data points:

$16 \text{ participants} \times 16 \text{ questions} \times 200 \text{ fNIRS}_{\text{points}} \times 16 \text{ optodes}$.

3.3 fNIRS Signal processing using fNIRSoft

After data acquisition, we applied following steps on our fNIRS signals using fNIRSoft software [1]. We checked raw light intensities and individual optodes visually. First, we rejected some noisy channels because of the failure to collect hemodynamic activity. It happened due to improper headband placement and contact between the sensors and the forehead. Next, we used a finite impulse response filter (20th order, Hamming window), a low pass filter, which removed the raw light intensity

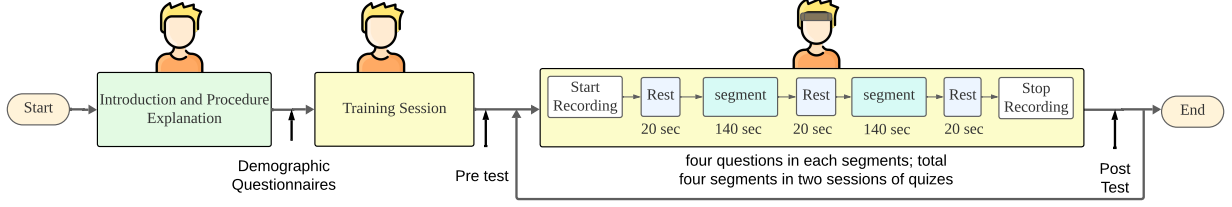


Figure 3: Overview of the study procedures: Participants began with consent, demographic surveys, and a demo. A 20-second resting baseline preceded each 140-second task segment (4 questions). Rest periods were added between segments and sessions. Pre- and post-tests were collected using Qualtrics.

data at 0.1 Hz input from physiological signals, such as respiration and heartbeat. Then we applied the Modified-Beer Lambert rule, where fNIRS transforms light intensity measurements into changes in the concentrations of ΔHbO [2, 3]. According to the rule, a light’s attenuation depends on the medium’s characteristics it passes through [2, 3]. A portion of the near-infrared light used in fNIRS is absorbed by hemoglobin in the blood arteries in the brain. oxygenated hemoglobin (ΔHbO) concentrations are associated with changes in brain activity. fNIRS calculates the changes in oxygenated hemoglobin, ΔHbO , by quantifying how much light is absorbed [2, 3]. Then, the detrending filter was applied to data characterizing changes in concentration to remove drift in the data using linear parameters that convert the baseline slope to zero. We got oxygenated hemoglobin ΔHbO from the available biomarkers sent by Python script [35, 36]. At the end, we labeled the data using fNIRSoft software and saved them in CSV file format. Later, we extracted the quiz responses based on filenames. Then, we handled missing values by imputing with the mean per question and cleaned column names to prevent errors.

3.4 Feature Extraction Framework

The dataset contained fNIRS-derived ΔHbO signals from 16 optodes, including: *Physiological data*: optical density measurements (Optode 1-16); *Experimental metadata*: participant ID, question ID, question order, session; *Labels*: binary correct/incorrect answers. First, we identified optode-specific columns (Optode 1–16). For each optode, we computed Statistical Features (ST) and Functional Connectivity (FC).

Statistical Features (ST): $16 \times 8 = 128$ statistical features (ST) were derived per optode which includes mean, standard deviation, maximum, minimum, gradient mean, squared gradient mean, skewness, and kurtosis.

Functional Connectivity (FC) Features: For each question, we computed a 16×16 Pearson correlation matrix using the 200-timepoint ΔHbO signals from all 16 optodes. These pairwise correlations capture functional connectivity between brain regions. To avoid redundancy, we

extracted the 120 unique values from the upper triangle of the matrix (excluding the diagonal) as FC features.

Temporal Feature Engineering: Next, to capture temporal dynamics across the task, we computed delta (Δ) features by subtracting the features of question Q_{n-1} from Q_n for each participant. This was done separately for both ST and FC features, resulting in ΔST and ΔFC features. These deltas reflect changes in local brain activity and inter-regional connectivity between successive questions.

First, Data was sorted by Participant and Question_order. For each participant, temporal changes, Δ -features for ST and FC were computed as:

$$\Delta feature = Feature_{Q_n} - Feature_{Q_{n-1}} \quad (5)$$

To understand which brain regions most contribute to performance prediction, we analyzed temporal changes (Δ features) in ST and FC features across PFC subregions. FC captures how different brain regions interact over time. Changes in FC reflect network-level reconfiguration, which is critical for performance after break or task switch.

3.5 Model Architecture

To evaluate our model, we compute precision, recall, and F1-score. Precision measures the proportion of correctly predicted positive observations to the total predicted positive observations. Recall evaluates the proportion of correctly predicted positive observations to all actual positive observations. A high recall indicates the model successfully captures most of the positive instances. F1-score is the harmonic mean of precision and recall. It is particularly useful when the class distribution is imbalanced. To evaluate whether ML can reliably predict performance from fNIRS-derived features, we assessed multiple classifiers (e.g., Logistic Regression, SVM, Random Forest) across five types of features (Basic, statistical features (ST), Functional Connectivity (FC), ST+FC, and Temporal). Before training the models, we applied standardization (Z-score normalization) to ensure uniform feature scaling. Finally, we used 5-fold cross-validation by applying GroupKFold $n_splits = 5$

to ensured participant-independent splits. Each fold consisted of a participant-wise split to ensure no overlap between train and test participants. Specifically, in each fold, approximately 80% of participants (13 or 12 out of 16) were used for training and the remaining 20% (3 or 4) for testing. This setup ensured participant-independent evaluation and avoided data leakage across folds.

These features are then used as input for various classification algorithms. Five different classifiers are used independently within a 5-fold stratified cross-validation framework: Logistic Regression (LR), SVM (RBF Kernel), K-Nearest Neighbors (KNN, $k=5$), Linear discriminant analysis (LDA), Decision Tree (DT), Random Forest (RF), XGBoost. The output of the classification is a binary prediction of correct (1) or incorrect (0) response.

4 Results

4.1 Model Evaluation

From Table 1, we can see that while the models achieved prediction accuracies ranging from 58% to 67%, which is above the random baseline, the performance suggests room for improvement in model robustness and feature refinement. For instance, the Random Forest classifier achieved an accuracy of 67% with ST+FC features, while SVM shows consistent performance across (62%-65%) feature types. Recall remained consistently moderate-to-high (up to 0.68) and indicates that the models were able to correctly identify a substantial proportion of correct and incorrect answer. These findings collectively demonstrate that ML models can feasibly predict task performance from brain signal-derived features, without relying on any specific model being best. No statistically significant differences were found between classifiers (*Wilcoxon*, $p > 0.05$). This supports our focus on interpretability over performance optimization. The consistency across models suggests that fNIRS features encode robust cognitive signals that can be captured similarly by different classifiers. We also applied deep learning models such as CNN (60.05%), GRU (63.75%), LSTM (64.68%), and BiLSTM (63.43%) models. However, due to the limited size of our dataset—only 256 samples (16 participants \times 16 questions)—the models tended to overfit, and validation accuracy did not significantly improve over traditional ML methods. The relatively high parameter count of DL architectures, combined with the small dataset, hindered generalization, which aligns with past findings on DL sensitivity to data volume in neuroimaging studies.

4.2 Estimation of Cognitive Effort

In this study, our focus was to find if predicted score using AI, can be helpful to estimate cognitive effort. To represent cognitive effort we have calculated relative neural efficiency (RNE) and neural involvement (RNI)

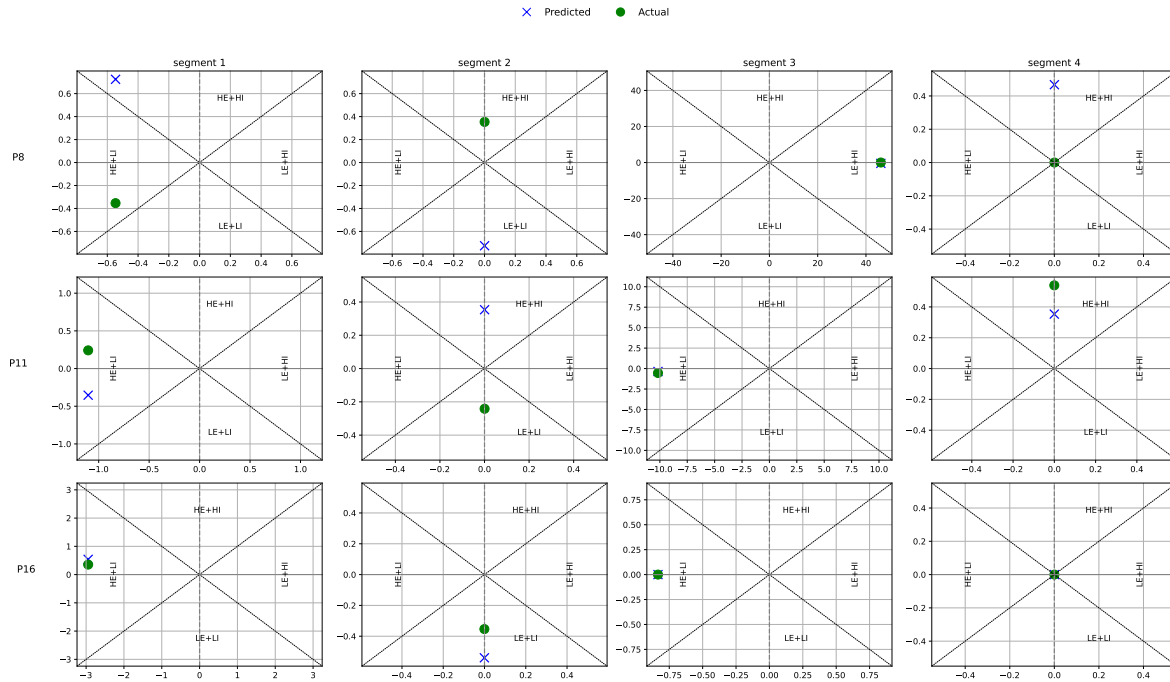
using equation 4. These metrics provided a deeper understanding of participants' cognitive states across task segments. We selected one test case that included three participants: P8, P11, and P16. we quantified similarity using Mean Absolute Error (MAE) and Pearson correlation actual and predicted RNE and RNI values across task segments for three test participants. The very low MAE (0.29 for RNE and 0.38 for RNI) and near-perfect correlation $r = 0.999$ suggest strong alignment that the model's predicted RNE and RNI values closely follow the actual measurements.

To understand participants' efficiency and involvement we plotted Z-score standardized $\Delta HbOM_Z$ in X axis and Z-score standardized performance score P_z in Y axis. Figure 4 shows participant-wise RNE and RNI in a Cartesian plot. The diagonal from bottom-left to top-right marks the efficiency line—points above indicate high neural efficiency. The opposite diagonal represents involvement—points above it indicate high neural involvement. This divides the space into four cognitive states: HE+HI (High Efficiency, High Involvement), HE+LI (High Efficiency, Low Involvement), LE+HI (Low Efficiency, High Involvement), and LE+LI (Low Efficiency, Low Involvement). Predicted coordinates are plotted alongside actual values for participants P8, P11, and P16 across four task segments.

Out of the 12 predicted coordinates, 9 matched the actual cognitive states when visualized in the RNE-RNI Cartesian plot. Although the accuracies of the machine learning models are moderate, the plotting suggests strong interpretability in terms of cognitive state estimation. In our framework, RNE and RNI are evaluated not only by their values but also by their relative position and distance from the efficiency and involvement diagonals. Therefore, even when the exact predicted RNE/RNI values deviate from ground truth, the quadrant-wise agreement in most cases suggests that the model captures broad cognitive states rather than precise individual metrics. In segment 1, all participants showed low neural efficiency but varied involvement which often associated with the early learning phase. Segment 2 showed clustering near the origin for most participants, implying a moderate-effort transitional state. Segment 3 revealed decreased effort for P11 and P16, possibly prompting the subsequent long break. P8, who reported a headache after segment 2, exhibited higher cognitive effort in segment 3. Finally, in segment 4, cognitive effort generally declined again after a short rest, with participants transitioning toward lower-effort zones. These results highlight that our model's predictions are cognitively meaningful, even when numeric prediction errors exist, supporting its utility for estimating learner state in real-time applications.

Table 1: Performance Comparison of Machine Learning Models. Higher represents better. Accuracy ranges from 58% to 67%

Feature	Metric	LR	SVM	KNN	LDA	DT	RF	XGBoost
Basic	Accuracy	0.65	0.65	0.57	0.65	0.53	0.63	0.58
	Precision	0.53	0.46	0.53	0.53	0.51	0.58	0.54
	Recall	0.65	0.65	0.57	0.65	0.53	0.63	0.58
	F1 Score	0.56	0.52	0.54	0.57	0.52	0.59	0.54
ST	Accuracy	0.55	0.65	0.58	0.51	0.52	0.62	0.62
	Precision	0.55	0.43	0.55	0.53	0.54	0.58	0.61
	Recall	0.55	0.65	0.58	0.51	0.52	0.62	0.62
	F1 Score	0.53	0.52	0.54	0.52	0.52	0.57	0.60
FC	Accuracy	0.55	0.62	0.58	0.53	0.48	0.61	0.58
	Precision	0.57	0.45	0.54	0.58	0.50	0.61	0.55
	Recall	0.55	0.62	0.58	0.53	0.48	0.61	0.58
	F1 Score	0.55	0.51	0.55	0.54	0.49	0.56	0.56
ST+FC	Accuracy	0.56	0.64	0.58	0.51	0.53	0.67	0.65
	Precision	0.58	0.52	0.59	0.58	0.54	0.65	0.63
	Recall	0.56	0.65	0.58	0.51	0.53	0.67	0.65
	F1 Score	0.56	0.53	0.56	0.52	0.54	0.61	0.62
Temporal	Accuracy	0.62	0.64	0.65	0.50	0.66	0.56	0.59
	Precision	0.63	0.68	0.63	0.57	0.68	0.59	0.57
	Recall	0.62	0.64	0.65	0.50	0.66	0.56	0.59
	F1 Score	0.62	0.55	0.56	0.52	0.61	0.56	0.54

**Figure 4: Cartesian representation of predicted vs. actual cognitive states. X-axis: standardized ΔHbO (M_Z); Y-axis: standardized performance score (P_Z). Circles = actual scores; crosses = predicted scores. Quadrants represent cognitive states: HE+HI (High Efficiency, High Involvement), HE+LI, LE+HI, LE+LI.**

5 Discussion

The aim of this study is to estimate cognitive effort during educational tasks by analyzing fNIRS-derived hemodynamic responses and predicted performance scores. Our findings highlight that model predictions, even with moderate accuracy, can reveal meaningful cognitive trends when analyzed through RNE and RNI. We used various machine learning models to predict quiz performance from brain signals and then we derived Relative Neural Efficiency (RNE) and Relative Neural Involvement (RNI) to interpret learner efficiency and involvement. The contribution of this work is that it shows that cognitive effort can be meaningfully measured using a combination of brain signals and machine learning-based performance prediction. These findings might influence future adaptive learning systems.

For RQ_1 : The results of this study demonstrate that task performance prediction using fNIRS-derived brain features is not only feasible but also effective across a variety of feature types and classifiers. While our focus was not on identifying the single best-performing model, the consistent performance across classifiers confirms that fNIRS signals—especially when processed into spatial, functional, or temporal representations—contain rich cognitive information. The strong model generalization across ST, FC, and delta (Temporal) features highlights that both static brain activation and dynamic changes during tasks contribute meaningfully to performance estimation. There was no statistically significant performance difference. This consistency suggests that the cognitive patterns embedded in fNIRS signals are inherently stable and interpretable, regardless of the specific model architecture.

For RQ_2 , these derived measures help interpret learners' cognitive effort, involvement, and efficiency during educational gameplay. Even with moderate accuracy, the predicted CE trends followed actual RNE/RNI patterns. Since we use aggregated and z-scored values for CE estimation, occasional false positives/negatives have a limited impact on the overall cognitive state trends. The derived RNE/RNI values smooth out individual prediction errors. Also, to observe cognitive effort patterns, we used a Cartesian plot. We observed the predicted values most of the time were aligned with the actual values in the same quadrant of the Cartesian plot. This spatial overlap indicates that the model was able to capture similar patterns of cognitive effort behavior. Therefore, the proposed model not only supports cognitive effort estimation but also aids in the interpretation of cognitive state trends across different learning segments.

However, future improvements can reduce this noise further. Our goal was not to maximize classification accuracy alone, but to enable interpretable CE estimation using RNE and RNI. We plan to explore more robust or adaptive machine and deep learning architectures in

future work. Cognitive effort is highly individualized. While our model captures general trends, it does not yet account for individual baselines or variability in fNIRS responses. Adaptive or personalized calibration may improve robustness in future work.

6 Conclusion

This study demonstrates a method for estimating and interpreting cognitive effort through performance scores predicted by various machine learning models and oxygenated hemoglobin (ΔHbO) in the brain collected using fNIRS. This work demonstrates that AI models can support interpretable cognitive effort estimation, going beyond performance to inform adaptive learning design. Our findings confirm that ML-predicted performance, combined with fNIRS data, provides a viable estimate of neural efficiency and involvement. We observed the positive correlation between the brain feature dynamics and performance score in an educational game. This predicted score was used to estimate cognitive effort by measuring relative neural efficiency and involvement. The machine learning models showed accuracy ranges from 58% to 67%. After estimating RNE and RNI, we observed that the mean absolute error is very low between actual and predicted RNE/RNI values, which suggests that predicted RNE and RNI closely follow the actual RNE and RNI. This approach paves the way for a personalized educational setup that can dynamically adapt to learners' cognitive states, potentially adjusting to classroom and remote educational settings. By deriving RNE and RNI from predicted performance and effort, we show meaningful trends tied to cognitive states. The findings highlight the model's potential in adaptive learning contexts and highlight future directions in real-time neuro-adaptive systems.

References

- [1] Biopac Systems Inc. [n. d.]. fNIRSoft Professional Edition. Software; retrieved from Biopac website. <https://www.biopac.com/product/fnirsoft-professional-edition/> Accessed July 17, 2025.
- [2] Murat Perit Cakir, Nur Akkuş Çakir, Hasan Ayaz, and Frank J Lee. 2015. An optical brain imaging study on the improvements in mathematical fluency from game-based learning. In *Proceedings of the 2015 Annual Symposium on Computer-Human Interaction in Play*. 209–219.
- [3] Murat Perit Çakır, Nur Akkuş Çakır, Hasan Ayaz, and Frank J Lee. 2016. Behavioral and neural effects of game-based learning on improving computational fluency with numbers: An optical brain imaging study. *Zeitschrift für Psychologie* 224, 4 (2016), 297.
- [4] Antonio Maria Chiarelli, Pierpaolo Croce, Arcangelo Merla, and Filippo Zappasodi. 2018. Deep learning for hybrid EEG-fNIRS brain-computer interface: application to motor imagery classification. *Journal of neural engineering* 15, 3 (2018), 036028.
- [5] Pietro A. Cicalese, Rihui Li, Mohammad B. Ahmadi, Chushan Wang, Joseph T. Francis, Sudhakar Selvaraj, Paul E. Schulz, and Yingchun Zhang. 2020. An EEG-fNIRS hybridization technique in the four-class classification of alzheimer's disease. *Journal of Neuroscience Methods* 336 (2020), 108618. doi:10.1016/j.jneumeth.2020.108618

- [6] Ciaran Cooney, Raffaella Folli, and Damien Coyle. 2022. A Bimodal Deep Learning Architecture for EEG-fNIRS Decoding of Overt and Imagined Speech. *IEEE Transactions on Biomedical Engineering* 69, 6 (2022), 1983–1994. doi:10.1109/TBME.2021.3132861
- [7] Javier De La Cruz, Douglas Shimizu, and Kiran George. 2022. EEG and fNIRS Analysis Using Machine Learning to Determine Stress Levels. In *2022 IEEE World AI IoT Congress (AIoT)*. 318–322. doi:10.1109/AIoT54504.2022.9817318
- [8] Aykut Eken, Murat Yüce, Gülnaz Yükselen, and Sinem Burcu Erdoğan. 2024. Explainable fNIRS-based pain decoding under pharmacological conditions via deep transfer learning approach. *Neurophotonics* 11, 4 (2024), 045015–045015.
- [9] Raul Fernandez Rojas, Calvin Joseph, Ghazal Bargshady, and Keng-Liang Ou. 2024. Empirical comparison of deep learning models for fNIRS pain decoding. *Frontiers in Neuroinformatics* 18 (2024), 1320189.
- [10] Sabrina Gado, Katharina Lingelbach, Maria Wirzberger, and Mathias Vukelić. 2023. Decoding Mental Effort in a Quasi-Realistic Scenario: A Feasibility Study on Multimodal Data Fusion and Classification. *Sensors* 23, 14 (2023). doi:10.3390/s23146546
- [11] Nancy Getchell and Patricia Shewokis. 2023. Understanding the role of cognitive effort within contextual interference paradigms: Theory, measurement, and tutorial. *Brazilian Journal of Motor Behavior* 17, 1 (2023), 59–69.
- [12] Nicolas Grimaldi, David Kaber, Ryan McKendrick, and Yunmei Liu. 2024. Deep Learning Forecast of Perceptual Load Using fNIRS Data. *Human Factors in Design, Engineering, and Computing* 159, 159 (2024).
- [13] Nicolas Grimaldi, Yunmei Liu, Ryan McKendrick, Jaime Ruiz, and David Kaber. 2024. Deep Learning Forecast of Cognitive Workload Using fNIRS Data. In *2024 IEEE 4th International Conference on Human-Machine Systems (ICHMS)*. 1–6. doi:10.1109/ICHMS59971.2024.10555701
- [14] Edgar Guevara, Gabriel Solana-Lavalle, and Roberto Rosas-Romero. 2024. Integrating fNIRS and machine learning: shedding light on Parkinson's disease detection. *EXCLI journal* 23 (2024), 763.
- [15] Yang Gui, Zhihui Cai, Si Zhang, and Xitao Fan. 2025. Dyads composed of members with high prior knowledge are most conducive to digital game-based collaborative learning. *Computers & Education* 230 (2025), 105266. doi:10.1016/j.compedu.2025.105266
- [16] Nazo Haroon, Hamid Jabbar, Umar Shahbaz, Taikyeong Jeong, and Noman Naseer. 2024. Mental Fatigue Classification Aided by Machine Learning-Driven Model under the Influence of Foot and Auditory Binaural Beats Brain Massage Via fNIRS. *IEEE Access* (2024).
- [17] M Hasan, M Mahmud, S Poudel, K Donthula, and K Poudel. 2023. Mental Workload Classification from fNIRS Signals by Leveraging Machine Learning. In *2023 IEEE Signal Processing in Medicine and Biology Symposium (SPMB)*. IEEE, 1–6.
- [18] Hina Jabbar, Noman Naseer, and Adil Saeed. 2020. Enhancing information transfer rate of multi-class BCI system by improving classification accuracies using machine learning methods. In *Proceedings of the 13th ACM International Conference on Pervasive Technologies Related to Assistive Environments (Corfu, Greece) (PETRA '20)*. Association for Computing Machinery, New York, NY, USA, Article 3, 4 pages. doi:10.1145/3389189.3393746
- [19] Yu Jin Jeun, Yunyoung Nam, Seong A Lee, and Jin-Hyuck Park. 2022. Effects of Personalized Cognitive Training with the Machine Learning Algorithm on Neural Efficiency in Healthy Younger Adults. *International Journal of Environmental Research and Public Health* 19, 20 (2022). doi:10.3390/ijerph192013044
- [20] Haroon Khan, Farzan M. Noori, Anis Yazidi, Md Zia Uddin, M. N. Afzal Khan, and Peyman Mirtaheri. 2021. Classification of Individual Finger Movements from Right Hand Using fNIRS Signals. *Sensors* 21, 23 (2021). doi:10.3390/s21237943
- [21] Jaewon Kim, Hayeon Lee, Jinseok Lee, Sang Youl Rhee, Jae Il Shin, Seung Won Lee, Wonyoung Cho, Chanyang Min, Rosie Kwon, Jae Gwan Kim, and Dong Keon Yon. 2023. Quantification of identifying cognitive impairment using olfactory-stimulated functional near-infrared spectroscopy with machine learning: a post hoc analysis of a diagnostic trial and validation of an external additional trial. *Alzheimer's Research & Therapy* 15, 1 (2023), 127. doi:10.1186/s13195-023-01268-9
- [22] Reza Koiler, Austin Schimmel, Elham Bakhshipour, Patricia A Shewokis, and Nancy Getchell. 2022. The impact of fidget spinners on fine motor skills in individuals with and without ADHD: An exploratory analysis. *Journal of Behavioral and Brain Science* 12, 3 (2022), 82–101.
- [23] Lin Li, Jingxuan Liu, Yifan Zheng, Chengchao Shi, and Wenting Bai. 2025. Identification of Subthreshold Depression Based on fNIRS-VFT Functional Connectivity: A Machine Learning Approach. *Depression and Anxiety* 2025, 1 (2025), 7645625.
- [24] Jieqiong Liu, Ruqian Zhang, Binbin Geng, Tingyu Zhang, Di Yuan, Satoru Otani, and Xianchun Li. 2019. Interplay between prior knowledge and communication mode on teaching effectiveness: Interpersonal neural synchronization as a neural marker. *NeuroImage* 193 (2019), 93–102. doi:10.1016/j.neuroimage.2019.03.004
- [25] Pei Ma, Chenyang Pan, Huijuan Shen, Wushuang Shen, Hui Chen, Xuedian Zhang, Shuyu Xu, Jingzhou Xu, and Tong Su. 2025. Monitoring nap deprivation-induced fatigue using fNIRS and deep learning. *Cognitive Neurodynamics* 19, 1 (2025), 30. doi:10.1007/s11571-025-10219-z
- [26] Tengfei Ma, Wentian Chen, Xin Li, Yuting Xia, Xinhua Zhu, and Sailing He. 2021. fNIRS Signal Classification Based on Deep Learning in Rock-Paper-Scissors Imagery Task. *Applied Sciences* 11, 11 (2021). doi:10.3390/app11114922
- [27] Amanda Yumi Ambriola Oku and João Ricardo Sato. 2021. Predicting Student Performance Using Machine Learning in fNIRS Data. *Frontiers in Human Neuroscience* 15 (2021). doi:10.3389/fnhum.2021.622224
- [28] Pablo Ortega and A Aldo Faisal. 2021. Deep learning multimodal fNIRS and EEG signals for bimanual grip force decoding. *Journal of neural engineering* 18, 4 (2021), 0460e6.
- [29] Fred Paas, Alexander Renkl, and John Sweller. 2003. Cognitive load theory and instructional design: Recent developments. *Educational psychologist* 38, 1 (2003), 1–4.
- [30] Yafeng Pan, Suzanne Dikker, Pavel Goldstein, Yi Zhu, Cuirong Yang, and Yi Hu. 2020. Instructor-learner brain coupling discriminates between instructional approaches and predicts learning. *NeuroImage* 211 (2020), 116657. doi:10.1016/j.neuroimage.2020.116657
- [31] Yafeng Pan, Giacomo Novembre, Bei Song, Xianchun Li, and Yi Hu. 2018. Interpersonal synchronization of inferior frontal cortices tracks social interactive learning of a song. *NeuroImage* 183 (2018), 280–290. doi:10.1016/j.neuroimage.2018.08.005
- [32] Sara Quattrocchi, Arcangelo Merla, Daniela Cardone, and David Perpetuini. 2024. Advanced Machine Learning Approaches for Classifying Parkinson's Disease Using fNIRS Data from Gait Analysis. In *2024 E-Health and Bioengineering Conference (EHB)*. 1–4. doi:10.1109/EHB64556.2024.10805716
- [33] Pratusha Reddy, Patricia A Shewokis, and Kurtulus Izzetoglu. 2022. Individual differences in skill acquisition and transfer assessed by dual task training performance and brain activity. *Brain informatics* 9, 1 (2022), 9.
- [34] Manob Jyoti Saikia. 2023. K-means clustering machine learning approach reveals groups of homogeneous individuals with unique brain activation, task, and performance dynamics using fNIRS. *IEEE Transactions on Neural Systems and Rehabilitation Engineering* 31 (2023), 2535–2544.
- [35] Shayla Sharmin and Md Fahim Abrar. 2025. *Python GUI Tool for Fixed-Time Automatic Keyboard Marker Sending in fNIRS Experiments (Alternative to PsychoPy)*. doi:10.5281/zenodo.15880996
- [36] Shayla Sharmin, Md Fahim Abrar, and Roghayeh Leila Barmaki. 2024. From Complexity to Simplicity: Using Python Instead of PsychoPy for fNIRS Data Collection. *arXiv preprint arXiv:2411.06523* (2024).
- [37] Shayla Sharmin, Elham Bakhshipour, Behdokht Kiafar, Md Fahim Abrar, Pinar Kullu, Nancy Getchell, and

- Roghayeh Leila Barmaki. 2025. Functional Near-Infrared Spectroscopy (fNIRS) Analysis of Interaction Techniques in Touchscreen-Based Educational Gaming. In *Proceedings of the 27th International Conference on Multimodal Interaction (ICMI '25)*. ACM, Canberra, ACT, Australia. doi:10.1145/3716553.3750811
- [38] Shayla Sharmin, Reza Koiler, Rifat Sadik, Arpan Bhattacharjee, Priyanka Raju Patre, Pinar Kullu, Charles Hohensee, Nancy Getchell, and Roghayeh Leila Barmaki. 2024. Cognitive Engagement for STEM+C Education: Investigating Serious Game Impact on Graph Structure Learning with fNIRS. In *2024 IEEE International Conference on Artificial Intelligence and eXtended and Virtual Reality (AIxVR)*. IEEE, 195–204.
- [39] Shayla Sharmin, Gael Lucero-Palacios, Behdokht Kiafar, Md Fahim Abrar, Mohammad Al-Ratrout, Aditya Raikwar, and Roghayeh Leila Barmaki. 2024. A Scoping Review of Functional Near-Infrared Spectroscopy (fNIRS) Applications in Game-Based Learning Environments. *arXiv preprint arXiv:2411.02650* (2024).
- [40] Patricia A Shewokis, Hasan Ayaz, Lucian Panait, Yichuan Liu, Mashaal Syed, Lawrence Greenawald, Faiz U Shariff, Andres Castellanos, and D Scott Lind. 2015. Brain-in-the-loop learning using fNIR and simulated virtual reality surgical tasks: hemodynamic and behavioral effects. In *Foundations of Augmented Cognition: 9th International Conference, AC 2015, Held as Part of HCI International 2015, Los Angeles, CA, USA, August 2–7, 2015, Proceedings 9*. Springer, 324–335.
- [41] Jungpil Shin, Sota Konnai, Md. Maniruzzaman, Md. Al Mehedi Hasan, Koki Hirooka, Akiko Megumi, and Akira Yasumura. 2023. Identifying ADHD for Children With Coexisting ASD From fNIRS Signals Using Deep Learning Approach. *IEEE Access* 11 (2023), 82794–82801. doi:10.1109/ACCESS.2023.3299960
- [42] M. Asjid Tanveer, M. Jawad Khan, M. Jahangir Qureshi, Norman Naseer, and Keum-Shik Hong. 2019. Enhanced Drowsiness Detection Using Deep Learning: An fNIRS Study. *IEEE Access* 7 (2019), 137920–137929. doi:10.1109/ACCESS.2019.2942838
- [43] Rui Varandas, Rodrigo Lima, Sergi Bermúdez I Badia, Hugo Silva, and Hugo Gamboa. 2022. Automatic Cognitive Fatigue Detection Using Wearable fNIRS and Machine Learning. *Sensors* 22, 11 (2022). doi:10.3390/s22114010
- [44] Sajila D. Wickramaratne and Md Shaad Mahmud. 2021. A Deep Learning Based Ternary Task Classification System Using Gramian Angular Summation Field in fNIRS Neuroimaging Data. In *2020 IEEE International Conference on E-health Networking, Application & Services (HEALTHCOM)*. 1–4. doi:10.1109/HEALTHCOM49281.2021.9398993
- [45] Chenyang Zhang, Chaozhe Jiang, Yuanyi Xie, Shi Cao, Jiajun Yuan, Chuang Liu, Weiwei Cao, and Yaohua Li. 2024. Assessing Pilot Workload during Takeoff and Climb under Different Weather Conditions: A fNIRS-based Modelling using Deep Learning Algorithms. *IEEE Trans. Aerospace Electron. Systems* 00, XXXX (2024), 1–23. doi:10.1109/TAES.2024.3458954
- [46] Yao Zhang, Dongyuan Liu, Tieni Li, Pengrui Zhang, Zhiyong Li, and Feng Gao. 2023. CGAN-rIRN: a data-augmented deep learning approach to accurate classification of mental tasks for a fNIRS-based brain-computer interface. *Biomed. Opt. Express* 14, 6 (Jun 2023), 2934–2954. doi:10.1364/BOE.489179
- [47] Hongyi Zhao, Jiangyu Chen, and Yiqi Lin. 2021. Intelligent recognition of hospital image based on deep learning: the relationship between adaptive behavior and family function in children with ADHD. *Journal of Healthcare Engineering* 2021, 1 (2021), 4874545.

Received ; revised ; accepted